DEPARMENT OF PHYSICS, UNIVERSITY OF JYVÄSKYLÄ
RESEARCH REPORT No. 1/1977

# A STUDY OF THE HELIUM-JET RECOIL-TRANSPORT METHOD AND ITS APPLICATION TO ON-LINE ISOTOPE SEPARATION

BY
JUHA ÄYSTÖ

Academic Dissertation
for the Degree of
Doctor of Philosophy

Jyväskylä Finland
March 1977

ISBN 951-677-777-5

DEPARMENT OF PHYSICS, UNIVERSITY OF JYVÄSKYLÄ
RESEARCH REPORT No. 1/1977

# A STUDY OF THE HELIUM-JET RECOIL-TRANSPORT METHOD AND ITS APPLICATION TO ON-LINE ISOTOPE SEPARATION

BY

JUHA ÄYSTÖ

Academic Dissertation
for the Degree of
Doctor of Philosophy

To be presented, by permission of the
Faculty of Mathematics and Natural Sciences
of the University of Jyväskylä
for Public examination in Auditorium II-212 of the
University of April 2, 1977, at 12 o'clock noon.

Jyväskylä Finland
March 1977

URN:ISBN:978-951-39-8540-0
ISBN 978-951-39-8540-0 (PDF)
ISSN 0075-465X

## Preface

It is a pleasure for me to express my sincere gratitude to my teacher, Professor Kalevi Valli. He has offered a wealth of ideas, continuous encouragement and support during the course of studies involved in the preparation of this thesis. Warm thanks are also due to Professor K. Eskola for all his advice and support.

My gratitude is due to Professor J. Kantele and Professor J. Hattula, for excellent working conditions at the Department of Physics of the University of Jyväskylä.

To my coworkers Dr. P. Puumalainen; Mr. K.-H. Hellmuth, Dipl. Chem.; Mr. J. Honkanen, M.Sc.; Mr. S. Hillebrand, M.Sc. and Mr. V. Rantala, Phil.Lic., I am greatly indebted.

Special thanks are due to Mr. T. Poikolainen, M.Sc., and Mr. R. Komu for their co-operation in the use of the cyclotron. The assistance of Mr. H. Leinonen and of the staff of the machine shop, Mr. A. Lyhty, Mr. P. Onkila and Mr. E. Liimatainen, is gratefully acknowledged. May I extend my thanks to all my other colleagues, as well.

I am obliged to Mr. T. Näränen for carefully finished drawings, to Mr. A. MacDougall, B.A., for revising the language of the manuscript and to Mrs. M. Selosmaa for the neat typing of this thesis.

I finally wish to thank my wife and my little daughter for their patience and unfailing support throughout my work.

For financial support I am indebted to the Academy of Finland, the University of Jyväskylä, Jenny ja Antti Wihurin rahasto ( Jenny and Antti Wihuri Foundation), Oskar Öflunds Stiftelse ( Oskar Öflund Foundation ) and to Emil Aaltosen säätiö ( Emil Aaltonen Foundation ).

Jyväskylä, February 1977

Juha Äystö

Contents

# A STUDY OF THE HELIUM-JET RECOIL-TRANSPORT METHOD AND ITS APPLICATION TO ON-LINE ISOTOPE SEPARATION


## Abstract

The helium-jet recoil-transport method and its coupling to the isotope separator on-line have been investigated. The dependence of the transport efficiency on several equipment parameters was studied both experimentally and theoretically. First, the transport efficiency of the He-jet method itself was studied. Pure commercial-grade helium, both at room temperature and at liquid nitrogen temperature, as well as carrier-loaded helium, was used. Efficiencies obtained with pure helium at room temperature were below 1 % when transport distances longer than one meter were used. Cooling of the helium down to liquid nitrogen temperature gave efficiencies of 10 - 50 % with several-meter transport distances. High transport efficiencies were also obtained when the helium was loaded with different carrier vapors. It was shown that additives have to form clusters with diameters from 0.01 - 1.0 μm for efficient transport of radioactivities. Next, a pure helium-jet at liquid nitrogen temperature coupled to a Nielsen type ion source, and a NaCl-loaded helium-jet coupled to a hollow cathode ion source, were investigated as means of connecting a cyclotron target chamber on-line to an isotope separator. Total separation efficiencies measured under various experimental conditions for several nuclides ( Cu, In, Sn, Sb, Ba, Bi ) were typically between 0.01 and 1.0 %.

## 1. Introduction

The helium-jet recoil-transport method[1] is well-known as a rapid means of transportation of radioactive reaction products from a helium-filled target chamber to a place outside the chamber where they can be studied. The aim is to bring the radioactivities away from the strong background radiation of the target chamber so that gamma-ray and particle spectroscopies can be carried out on them.

The principle of the method is shown diagramatically in fig. 1. Helium from a high pressure bottle flows through a rotameter

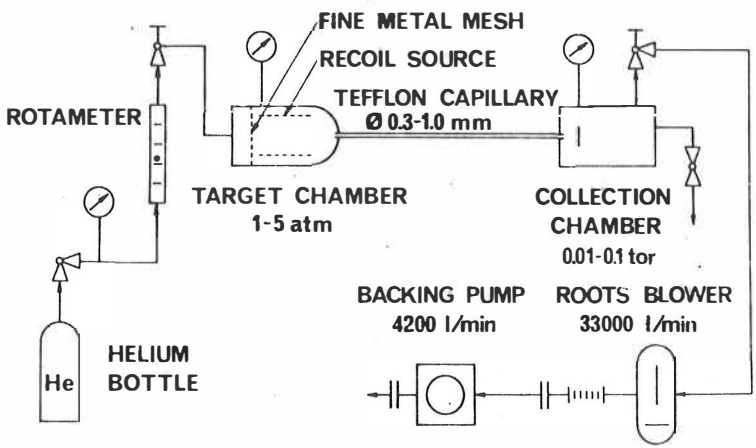


Fig. 1. Diagram of the helium-jet recoil-transport apparatus.

and a needle valve into a target chamber. The target chamber is connected to a collection chamber by means of a capillary. Low pressure is maintained in the collection chamber by means of a high-speed mechanical pump. The radioactive recoil atoms recoiling from the target or the source are stopped by the helium gas and are swept along with the helium through the capillary. They are deposited on a catcher foil or on a moving tape in the collection chamber.

The He-jet technique has been used for more than ten years as an aid in nuclear research, especially in the study of short-lived alpha-decaying nuclides[1-3]. In the early stage rather little attention was paid to the transport mechanism itself. However, the realization of the possibilities for a variety of promising applications[1,4-12] has resulted in the need for a deeper understanding of the laws governing the transport process[13-21].

The purpose of the present investigation was to develop a reliable and efficient He-jet system to be used as such and as an integral part of an on-line isotope separator system. First, the transport efficiency of the He-jet apparatus was studied with pure helium at room temperature[19]. The method appeared to be useful only for short transport distances. In subsequent studies it was found that helium had to be loaded with a proper carrier substance or cooled down to liquid nitrogen ($LN_2$) temperature to achieve efficient transport over distances longer than a few centimeters[20,21]. From the calculations of the transport properties it is shown that thermal diffusion of transported

particles plays a decisive role in the transport mechanism. Both the liquid nitrogen-cooled and carrier-loaded He-jet methods were tested under several experimental conditions and transport efficienciencies from 10 to 70 % were obtained for transport distances of several meters.

The coupling of the He-jet to the isotope separator[7-11] is a promising alternative to the existing on-line isotope separation methods[22-24]. A He-jet system can be selective with respect to chemical elements under special circumstances but normally all elements, nonvolatile as well as volatile, can be brought into the ion source with equal efficiency. In this work two different combinations of the He-jet and ion source were studied: One employing a pure He-jet at liquid nitrogen temperature connected to a Nielsen type ion source, and the other employing a NaCl-loaded He-jet in combination with a hollow cathode ion source. Under optimum conditions, transport efficiencies of about one per cent were achieved.

The He-jet transport system and the on-line isotope separator will be used for the study of the nuclear properties of short lived nuclei produced by means of a 90 cm cyclotron. The subject of this thesis is limited, however, to the description of certain technical details and the performance of the He-jet method and its coupling to the isotope separator. The study was carried out during the years 1971 - 1976 at the Department of Physics, University of Jyväskylä, Finland. Most of the experimental results in this work have been included in the following publications:

1. J. Äystö and K. Valli:
Transport efficiency of the helium-jet recoil-transport method with pure helium
Nucl. Instr. Meth. 111 (1973) 531

2. J. Äystö, P. Puumalainen and K. Valli:
The carrier-loaded helium-jet transport method
Nucl. Instr. Meth. 115 (1974) 65

3. J. Äystö, S. Hillebrand, K. Hellmuth and K. Valli:
Transport of recoil atoms in a stream of liquid air cooled pure helium
Nucl. Instr. Meth. 120 (1974) 163

4. J. Äystö, V. Rantala, K. Valli, S. Hillebrand, M. Kortelahti, K. Eskola and T. Raunemaa:
Efficiency of an on-line isotope separator system employing cooled and NaCl-loaded He-jet methods
Nucl. Instr. Meth. 139 (1976) 325

## 2. Theoretical

### 2.1. Flow characteristics

The problems of fluid dynamics in the He-jet system are associated with the gas flow from the target chamber into the capillary, with the flow through the capillary and with the expansion of the gas jet at the capillary exit and with its interaction with the catcher foil. While most of these problems are extremely complicated, the most important one, e.g. the flow through the capillary, allows a simplified theoretical treatment that provides at least a qualitative explanation of experimental results.

Let us assume a one dimensional viscous compressible flow through a constant area capillary in which there is no heat transfer. The variation of fluid properties along the axial path of the capillary can be derived from the equation of continuity, the equation of motion and the equation of state for an ideal gas. The variation of the local velocity in the capillary is given by the following formula[25] :

$$(1) \qquad 4C_f \frac{x}{D} = \frac{1}{\kappa}\left(\frac{1}{M_o^2} - \frac{1}{M^2}\right) + \frac{\kappa+1}{2\kappa} \ln\left[\frac{M_o^2}{M^2} \cdot \frac{1 + \frac{1}{2}(\kappa-1) M^2}{1 + \frac{1}{2}(\kappa-1) M_o^2}\right],$$

where

$C_f$ = friction factor,

$x$ = distance from the inlet of the capillary,

$D$ = diameter of the capillary,

$\kappa = c_p/c_v = 5/3$ for helium,

$c_p$ = specific heat at constant pressure,

$c_v$ = specific heat at constant volume,

$M = v/a$ = Mach number at a distance $x$,

$M_o = v_o/a$ = Mach number at inlet,

$v$ = velocity of helium,

$a$ = velocity of sound = $\sqrt{\kappa RT}$,

$R$ = gas constant for He,

$T$ = absolute temperature.

A good approximation of the inlet velocity is obtained simply by dividing the flow rate by the cross-sectional area of the capillary. This results in a few per cent inaccuracy in cases where the Mach number at inlet is of the order of 0.1. Similarly, the change in temperature and pressure between the target chamber and the capillary inlet is only a few per cent and is omitted in calculations. The maximum magnitude of the gas velocity in the capillary is a local velocity of sound. This can be explained[25] in terms of the maximum entropy at $M = 1.0$.

Assuming that the sonic velocity is reached at the end of the capillary, the velocity distribution along the capillary can be calculated from the formula[26] :

$$(2) \qquad \frac{1}{M} = \left[1 - \frac{x}{L}\right]^{\frac{1}{2}} \left[\frac{1 - M_o}{M_o}\right] + 1 \quad ,$$

where L is the length of a capillary. The magnitude of the velocity is obtained from the local Mach number as follows[25] :

$$(3) \qquad v = v_o \frac{M}{M_o} \left[ \frac{1 + \frac{\kappa-1}{2} M_o^2}{1 + \frac{\kappa-1}{2} M^2} \right]^{1/2} .$$

Formula (2) is an approximation to formula (1) and has been found to hold within 5 %. The total transport time is determined by the time spent in the target chamber and by the transmission time through the capillary. Expression (2) yields, for the transit time through the capillary[26],

$$(4) \qquad t = \frac{L}{a} \frac{(2 + M_o)}{3M_o} .$$

In practice the radial flow profile in a capillary is not constant as assumed in formulas (1), (2) and (3). In a fully developed laminar flow the radial profile has the form of a paraboloid. In this case the average velocity is a half of the maximum velocity at the capillary axis[25]. Assuming that the velocity distribution is uniform across the diameter at the capillary inlet, it reaches a parabolic profile at a distance of $L_e = 0.1 \times N_R \times R$. The symbol $N_R = \rho v D/\mu$ is the Reynolds number, where $D = 2R$ is the diameter of a capillary, v is the velocity of flowing helium, $\rho$ is the

density of helium and $\mu$ is the coefficient of viscosity. In the case of a laminar flow, the relation between the Reynolds number and the friction factor ( given in formula (1) ) is $C_f = 16/N_R$. It is generally accepted that the flow remains laminar when the Reynolds number is below 2300[27]. In this work the condition of laminarity is normally fulfilled.

The transmission time of transported particles through the capillary is an important parameter in the calculation of transport properties of the He-jet method. It has been shown that when the concentration of transported particles remains low, below 1 %, the difference between their velocity and the velocity of flowing helium is negligible[26]. In this work the concentration is normally considerably below 1 % and formula (4) can well be used in the calculation of the transmission time of transported particles through the capillary.

## 2.2. Losses in the transport line

There are several factors affecting the probability of transmission of a recoil atom through the He-jet system. Losses of radioactivity occur in the target chamber, at the capillary inlet, in the capillary and in the collection site. Experiments with pure helium as a transport gas have shown that the most critical part is the capillary. In a typical case more than 50 % of the produced activity can be adsorbed on the capillary walls[19].

The practical experience of several research groups has shown that certain impurities added to helium improve probability of transmission[1]. This improvement has been shown to be related to the size of the impurity particles and the temperature of the transport gas[14,16,20]. Even pure helium can transport recoil atoms with high efficiency when the whole system is operated at liquid nitrogen temperature[21]. These experimental findings indicate that losses in the transport system can largely be explained in terms of thermal diffusion and the gravitational movement of transported particles inside the capillary tube.

In the next two chapters a simple theoretical picture is given to explain the transmission of a particle with a given size and mass through the capillary. Later on, calculated transmission probabilities are compared to experimental ones ( chapters 3.2., 3.3. and 4.2.). The losses that occur inside

the target chamber, at the capillary inlet and on the catcher foil are not included in these calculations. Their share is qualitatively discussed in each specific case.

### 2.2.1. Diffusion

Thermal diffusion of particles in a capillary flow greatly depends on the radial velocity profile of the flow and on the nature of the flow, i.e. whether it is laminar or turbulent. As mentioned earlier, the flow in the He-jet system is generally laminar and has a radial profile of a parabolic form. Under these conditions the transmission through a capillary of radius R and length L is given approximately by the following expressions[28] :

(5) $$\frac{\bar{n}}{n_o} = 0.819 \cdot e^{-3.657\eta} + 0.097 \cdot e^{-22.3\eta} + 0.032 \cdot e^{-57\eta} + \ldots$$

$$( \eta > 0.04 )$$

or

(6) $$\frac{\bar{n}}{n_o} = 1 - 2.56\eta^{2/3} + 1.2\eta + 0.177\eta^{4/3} ,$$

$$( \eta \leq 0.04 )$$

where $n_o$ is the initial particle concentration and $\bar{n}$ is the mean concentration of particles at the capillary outlet. $\eta$ is a dimensionless quantity $(D \cdot L)/(R^2 \cdot \bar{v})$, where D is the diffusion

coefficient of particles in the transport gas and $\bar{v}$ the mean velocity of flow in the capillary.

In the case of a uniform radial velocity distribution, the transmission through a constant area tube is given by the following expansion of the squares of the zero-order Bessel functions of the first kind[28] :

$$(7) \qquad \frac{\bar{\bar{n}}}{n_o} = 4\left( \frac{1}{5.784} e^{-5.784\eta} + \frac{1}{30.47} e^{-30.47\eta} + \frac{1}{74.89} e^{-74.89\eta} + \ldots \right)$$

For small values of $\eta$ ( $\eta < 0.04$), i.e. in case of a small diffusion coefficient D, the difference between formula (7) and those for the parabolic flow is of the order of 10 %. In the case of large $\eta$ values the difference becomes significant. For example, with $\eta$ value of 0.5 the transmission given by formula (7) is 3.5 times lower than in the case of the parabolic flow.

In this work the diffusion coefficient is calculated separately for two kinds of particle. First, the diffusion coefficient for atomic particles is calculated on the basis of the molecular theory of gas mixtures[27]. Secondly, the diffusion coefficient for particles with a size comparable to, or larger than, the mean free path of gas molecules is calculated from the semiempirical formula given by Fuchs[28] as explained later on.

Let us assume that recoil atoms after thermalization behave like gaseous particles. The diffusion coefficient for a particle

with mass $m_1$ in a gas composed of molecules with mass $m_2$ is given by[27] :

$$(8) \qquad D = \frac{\sqrt{8\,k\,T}}{3\pi^{3/2}\, n\sigma_{12}^2 \sqrt{m}}$$

where

$k$ = Boltzman constant,
$T$ = absolute temperature of gas,
$n$ = number of gas molecules in $cm^3$,
$\sigma_{12} = \frac{1}{2}(\sigma_1 + \sigma_2)$ = average collision diameter,
$\sigma_1$ = (collision) diameter of a particle,
$\sigma_2$ = (collision) diameter of a gas molecule,
$m$ = reduced mass of $m_1$ and $m_2$.

It should be noted that the rms-distance, $\sqrt{\langle x^2 \rangle} = \sqrt{2\,D\,t}$, given by equation (8) is by a factor of five larger than that obtained from the elementary formula used in our previous study[21]. The formula for calculating the effect of temperature and pressure on the diffusion coefficient for atomic particles is as follows[27] :

$$(9) \qquad D_{T,p} = D\left(\frac{T}{288.2}\right)^{x} \frac{760}{P_{mmHg}} ,$$

where

$D_{T,p}$ = value at $T^{o}K$ and $P_{mmHg}$ ,

D = value at $288.2^{o}K$ and 760 mmHg.

The value of the experimental parameter x varies a little with the gas mixture but is generally close to 1.75.

The diffusion coefficient for particles with a size comparable to or larger than the mean free path of gas molecules is given by the formula[28] :

$$(10) \qquad D = \frac{k\,T}{6\pi\mu r}\left(1 + A\frac{l}{r} + Q\frac{l}{r}\,e^{-b\frac{r}{l}}\right),$$

where $\mu$ and l are the coefficient of viscosity and the mean free path of molecules of the transport gas. The diameter of a particle or a cluster is denoted by r. A, Q and b are experimental coefficients, the values of which depend mainly on the viscosity of the gas and the structure of the cluster surface. Values of A = 1.246, Q = 0.42 and b = 0.87 have been obtained for oil clusters in air[28]. Because the values of A, Q and b for helium and the cluster materials used in this work are not known, the values given for air and oil clusters were used in the transmission calculations in chapter 4.2.3.

### 2.2.2. Sedimentation

In horizontal tubes, the settling of clusters on capillary walls becomes significant when the cluster size exceeds a certain magnitude. The critical magnitude can be estimated from the settling velocity $V_s$ of clusters. The vertical velocity of a particle in a gas with viscosity $\mu$ under gravitational force is given by the expression[28] :

$$(11) \qquad V_s = \frac{2r^2 g\rho}{9\mu} \left( 1 + A \frac{1}{r} \right) ,$$

where r is the radius of the particle, $\rho$ is the density of the particle and g is the acceleration due to gravity. The experimental constant A is close to unity. The second term in the equation can be neglected because $1 \ll r$ in cases where settling on the walls is significant. Losses become significant when the particle radius is above 1.0 µm. The settling velocity for a particle with a diameter of 10 µm and a density of 1 g/cm$^3$ is about 1 cm/s. This means a distance of 1 mm in 100 ms, which is a typical flow-through rate for a capillary with a length of a few meters.

Assuming a parabolic flow profile, transmission through a horizontal tube under gravitational force is given by

the expression[28] :

$$(12) \quad \frac{n}{n_o} = 1 - \frac{2}{\pi} \left( 2K \sqrt{1-K^{2/3}} + \arcsin K^{1/3} - K^{1/3}\sqrt{1-K^{2/3}} \right) ,$$

where

$$K = \frac{3\ Vs\ L}{8\ R\ \bar{v}}$$

Complete adsorption occurs when K = 1, or when the transmission time through the capillary is longer than ( 8/3 )( $R/V_s$ ). For a uniform flow profile, the transmission is smaller, and in the case of large particles, can lead to losses at the inlet of the capillary[28].

# 3. Transport of recoil atoms with pure helium

## 3.1. Experimental

### 3.1.1. Recoil sources

Three different methods of recoil production were used in this work. Recoils were obtained from the alpha decay of $^{227}Ac$, from proton induced reactions, and from fission. Fission fragments from a $^{252}Cf$-source as well as from U-targets bombarded by protons and neutrons were used. More detailed data of the sources are given in table I.

The transport efficiency of the He-jet method is defined as the ratio of the number of counts measured from a catcher foil in the collection chamber to the number of counts measured from another foil placed directly on the recoil atom source.

The method of measuring transport efficiency as described above does not apply directly in the case of a $^{227}Ac$-source because of the gaseous decay product $^{219}Rn$. $^{227}Ac$ decays mainly via the following path:

$$\xrightarrow{\alpha} {}^{223}Ra \xrightarrow{\alpha} {}^{219}Rn \xrightarrow{\alpha} {}^{215}Po \xrightarrow{\alpha} {}^{211}Pb \xrightarrow{\beta^-} {}^{211}Bi \xrightarrow{\alpha}$$

11 d  4.0 s  1.8 ms  36 min  2.1 min

The long lived nuclide $^{227}Ac$ insures a practically constant

Table 1. Recoil production

| Means of production | Characteristics of the source |
|---|---|
| $^{227}$Ac-source | vacuum evaporated on Al-foil<br>strength ≈ 100 µC |
| (p,xn) reactions | metallic targets (Cu, Ni, Cd, Sn)<br>thickness ≈ 1 mg/cm$^2$ |
| $^{252}$Cf-source | electrodeposited on platinum disc<br>amount 2.5 µg<br>covered by one 1 mg/cm$^2$ gold foil |
| $^{nat.}$U (n,f) | metallic uranium on Ta backing<br>thickness 25 mg/cm$^2$ |
| $^{nat.}$U (p,f) | metallic uranium foil target<br>thickness 45 mg/cm$^2$ |

disintegration rate ( = recoil production rate ). The other α-active members from $^{219}Rn$ to $^{211}Bi$ are suitable for the measurement of transport properties. Because radon is not adsorbed onto a solid surface at room temperature and because the half-life of $^{215}Po$ is short compared to the flowthrough time of helium through the system ( 0.1 - 10 s ), it is mainly $^{211}Pb$ that is deposited on a catcher foil. Because a fraction of the 4.0 s $^{214}Rn$ flows out of the target chamber before disintegration, a correction is needed in determining the transport efficiency. If the measured $^{211}Bi$ activity on the catcher foil is a, then the activity $a_o$ corresponding to no $^{219}Rn$ escape is :

$$(13) \quad a_o \approx a/ ( 1 - e^{-\lambda t}) ,$$

where $\lambda = 0.173\ s^{-1}$ is the disintegration constant of $^{219}Rn$ and t is the average flowthrough time through the target chamber and the capillary. The flowthrough time through the target chamber is obtained by dividing the volume by the flow rate. The measuring time is assumed to be long compared to the half-life of $^{219}Rn$.

If not otherwise stated, the above α-activity measurements were performed off-line using collection and detection periods of 5 to 30 minutes. In the case of fission products, transport efficiencies were calculated from X-ray spectra or from known gamma transitions of certain fission products. Gamma transitions were also used in the case of charged particle induced reactions.

### 3.1.2. Apparatus used at room temperature

The apparatus was designed so that as many parameters as possible could be varied to find optimum conditions for efficient transport. The target chamber is an aerodynamically shaped metal cylinder with a teflon-surfaced interior. A fine metal mesh is placed across the chamber for the purpose of making the flow profile uniform. Two chambers, 28 $cm^3$ and 105 $cm^3$ in volume, were used. The $^{227}Ac$-source that was placed in the chamber was formed into a shape of a cylinder, the diameter of which was equal to that of the chamber. The catcher foil in the collection chamber was fixed to an adjustable holder that could be manipulated from outside. In other respects the equipment was as described in figure 1.

Attention was paid to the purity of the commercial grade helium that was used in the experiments. The purity of the helium gas was guaranteed by the supplier to be 99.998 % or better. Before entering the target chamber, the helium was passed through a cold trap filter that consisted of a spiral of copper tube immersed in liquid nitrogen. Later on, however, it was learned that a cold trap does not necessarily remove all impurities from helium[29]. Consequently, a series of tests was made without any filter, with a cold-trap filter, and with a ceramic filter that was known[29] to adsorb impurities. No essential difference in the transport properties was observed. On the other hand, small amounts of impurity ( > 100 ppm ) purposely mixed with helium increased transport efficiency dramatically.

### 3.1.3. Apparatus used at liquid nitrogen temperature

The characteristics of $LN_2$-cooled helium-jet transport were studied via three different systems, viz. with recoils from the $^{227}$Ac-source, with fission fragments from neutron induced fission, and with recoils from proton induced reactions. Later on, a $LN_2$-cooled $^{252}$Cf-source was constructed for the test purposes of an on-line isotope separator. Details of this source are given elsewhere[30].

a) The apparatus for the $^{227}$Ac-source

The apparatus is shown diagramatically in figure 2. The flow rate of helium is measured with a rotameter before entering a cooler. When required, a ceramic filter[29] and/or an active charcoal trap cooled with liquid nitrogen can be inserted between the high pressure helium bottle and the cooler. The cooler is a copper tube, of 4.5 mm internal diameter, submerged in liquid nitrogen. According to simple heat exchange estimates, about 1 m of the tube is required to lower the temperature of the flowing He-gas to within a few degrees of the temperature of liquid nitrogen. The lengths of our tubes were 3 - 10 m.

The recoil chamber is 2.5 cm in diameter and 9.5 cm long. It is made of brass, and sealed with a lead O-ring. The first part of the teflon capillary is enclosed in a tightly fitting copper tube and sealed with a neoprene O-ring. The temperature of the helium inside the chamber is measured with a thermocouple.

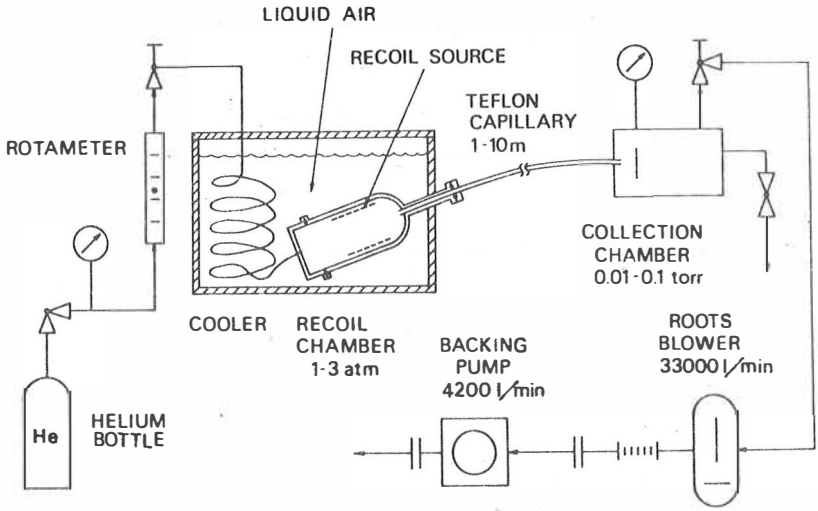


Fig. 2. Diagram of the He-jet recoil-transport apparatus cooled with liquid air or nitrogen.

Sometimes it is difficult to obtain a high transport yield without cooling the whole system, especially with transport distances of several meters. The properties of long capillaries

were investigated by winding them into circular coils of 0.5 m diameter and submerging the coils in liquid nitrogen.

b) The apparatus for neutron induced fission

In experiments with fission fragments, the experimental apparatus shown in fig. 2. was used. The recoil source was 25 mg/cm$^2$ of natural uranium on a tantalum backing placed a few millimeters behind the tritium target of the Sames 150 kV neutron generator. Because the density of helium is about 3.7 times higher at $LN_2$ temperature than at room temperature , a pressure of 2 atm in the recoil chamber is adequate to arrest all the recoiling fission fragments. Ranges of fission fragments in He vary between 2.1 and 2.6 mg/cm$^2$ [31], giving values of 1.5 - 2.0 cm at 2 atm and $LN_2$-temperature.

c) The apparatus for charged particle induced recoils

The target assembly placed in the cyclotron beam line is shown schematically in fig. 3.

The chamber was designed to be used both with a helium-jet cooled by liquid nitrogen and with a carrier-loaded helium-jet operated at room temperature. In studies with the $^{227}$Ac-source, it was found that both the source chamber and the initial length of the capillary must be carefully cooled for efficient transfer of activity[21]. Consequently, the space next to the reaction cell

is filled with $LN_2$, and the capillary can be cooled over its entire length by immersing it in $LN_2$. Prior to entering the target chamber the helium is precooled in a 2 m spiral shaped copper tube ( 5 mm i.d. ) placed inside the $LN_2$ container. The first 30 cm of the capillary ( i.d. 0.8 mm and wall thickness 0.1 mm ) leading from the reaction chamber to the collection site is of Cu-Ni alloy and the rest is of teflon. Lead O-rings are used as seals between different parts of the assembly.

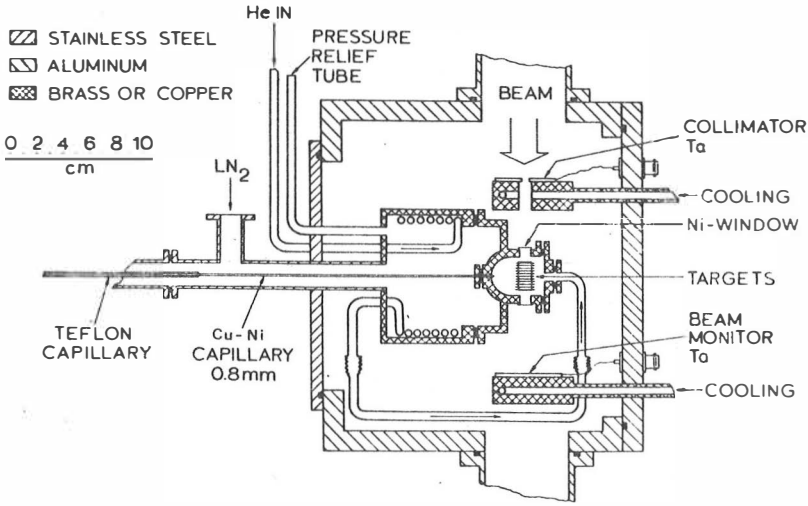


Fig. 3. Diagram of the target assembly. Detailed description is given in the text.

The beam enters the target chamber through a collimator and a 12 mg/cm$^2$ Ni window. The beam current is monitored by a water-cooled tantalum plate placed behind the exit window of the chamber. The estimated rise in temperature due to energy losses in windows and in the helium is a few degrees for 1 μA of 20 MeV protons. Several target foils can be stacked in the target holder placed inside the target chamber.

### 3.2. Results at room temperature

A number of measurements were made with the $^{227}$Ac-source to find out how much the transport efficiency depends on the length and the diameter of the capillary and on the pressure of the target chamber. These parameters define the flow properties of the system. On the other hand, the distance of the catcher foil from the capillary was varied to find the optimum collection efficiency for each flow. This was necessary because the adhesion of recoil atoms to the catcher foil depends strongly on the foil distance and the mass throughput of helium. The adhesion probability was found to be independent of the collection chamber pressure in the range 0.05 to 1.0 torr.

The results for capillaries of varying lengths and with an inner diameter of 0.8 mm are summarized in table II. The experimental transport efficiencies are corrected for the Rn escape

given by formula 13. For comparison, the calculated capillary transmissions are given in the last column.

Table II. Maximum transport efficiencies for capillaries with an inner diameter of 0.8 mm. The last column gives the theoretically calculated capillary transmission.

| Length of capillary (cm) | Pressure in target chamber (atm) | Flow rate $cm^3/s$ | Maximum efficiency (%) | Calculated capillary transmission (%) |
|---|---|---|---|---|
| 15 | 0.6 | 128 | 36 | 48.0 |
| 30 | 0.8 | 100 | 17 | 29.6 |
| 60 | 1.2 | 71 | 8.4 | 12.7 |
| 100 | 1.7 | 55 | 3.3 | 5.1 |

The Reynolds number with the parameters given above was between 1000 - 1200, indicating a laminar flow. The capillary transmission was calculated with the aid of formulas (5) and (8) given in chapter 2.2.1. In the calculation of the

diffusion coefficient, a collision diameter of 6 Å and a mass of 211 was assumed[21,27,32]. The collision diameter of a He atom was taken to be 2 Å[32]. The value of the diffusion coefficient was 0.32 $cm^2/s$ at the temperature of 293 K and the pressure of 1 atm.

The error in determining the experimental transport efficiency was typically ± 10 %. Calculated transmissions are consistently higher than experimentally determined efficiencies. The difference can be explained by the losses in the target chamber, at the capillary inlet, and on the catcher foil, that could not be taken into account in the calculations. Moreover, formula (5), where the parabolic flow profile was assumed, is not entirely valid. The parabolic flow profile is reached within the first 4 cm from the mouth of the capillary. For long capillaries, the effect of this developing distance is small. For capillaries with a length comparable to the developing distance the error that is made in calculations becomes significant as was shown in chapter 2.2.1. when comparing the transmissions of parabolic and uniform flows.

In order to obtain additional information the adsorption distribution in a capillary was measured[19]. The result is shown in fig. 4.

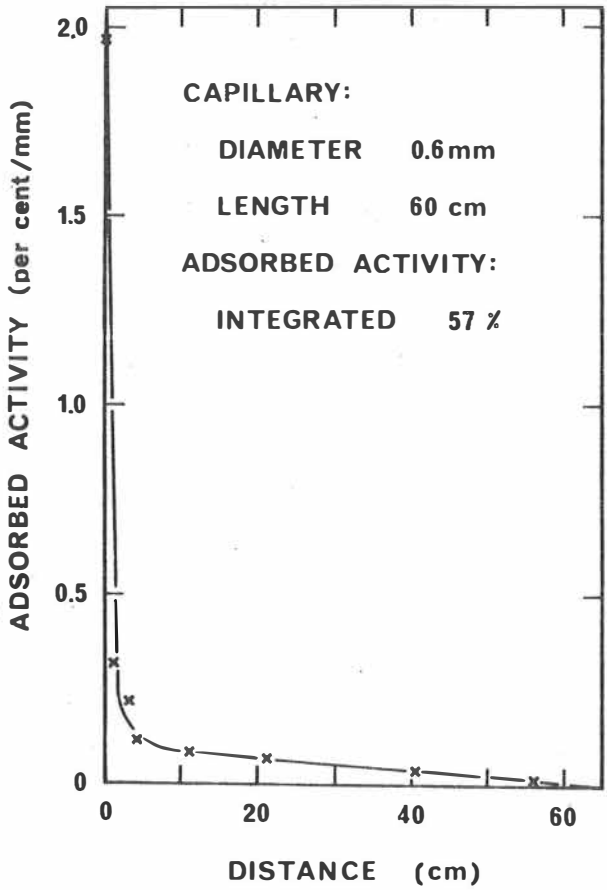


Fig. 4. Distribution of radioactivity adsorbed on the walls of the teflon capillary when transported by means of pure helium. The curve shown is meant only to assist in the reading of the figure.

The first two millimeters of the capillary were inside the target chamber. Thus the first point in the curve represents the sum of activities adsorbed both on the inner and the outer sides of the capillary. However, the form of the curve shows clearly the effect of the developing distance ( 4.5 cm ). In this case the transport efficiency on the catcher foil was about 4 %. Presumably most of the remaining 39 % is adsorbed into the target chamber walls.

On the basis of the considerations given above it is evident that the transmission formulae (5) and (6) are applicable in the case of atomic particles, i.e. in cases, where no carriers are used.

## 3.3. Results at $LN_2$ temperature

### 3.3.1. Total efficiency

A systematic study was performed to find out how far the transport efficiency depends on the length of the transport line, when the system is used at the temperature of liquid nitrogen. A considerable increase in the transport efficiency was achieved when the temperature of the system was lowered to the value of about 80 K. These measurements were made with recoils from the $^{227}$Ac-source. The results were confirmed

with recoils from (p,xn) reactions and with fission fragments. A summary of the results is given in table III.

The pressure and the flow rate of the helium were measured at room temperature ($\approx 20^{o}C$ ) before going to the cooler and the target chamber ( see fig. 2. ). The flow rate through the target chamber was obtained by multiplying the measured value by the ratio of the temperatures. With the capillaries, and the parameters given in table III, the Reynolds number was typically over 3000. However, the flow was assumed to be close to laminar, because only a smooth change in the transport efficiency was observed when the critical value of the Reynolds number (= 2300) was exceeded[21].

As discussed in chapter 3.1.1. a considerable fraction of $^{219}Rn$ recoil atoms may escape from the recoil chamber through the capillary before they decay by alpha-decay into $^{215}Po$. At room temperature radon is not adsorbed onto the catcher foil. The efficiencies corresponding to uncooled capillaries were corrected for radon escape using formula (13). In the case of cooled capillaries, the temperature of the catcher foil was found by measurement to be lower than the melting point of radon ( $-71^{o}C$ ) and the correction was omitted.

The capillary transmission for a particle with A = 211 and a diameter of 6 Å was calculated only in well defined cases, i.e. in cases where the whole system including the full length of the capillary was cooled with liquid nitrogen. The diffusion coefficient was calculated from formulas (8) and (9). The capillary transmission

Table III. Results obtained with the $LN_2$-cooled He-jet apparatus. Table gives maximum efficiencies for different transport distances. The last column gives the theoretically calculated capillary transmission.

| Length of capillary (m) | Diameter of capillary (mm) | Capillary cooled | Pressure in target chamber (atm) | Flow rate (at T=80 K) ($cm^3/s$) | Maximum efficiency (%) | Calculated capillary transmission (%) |
|---|---|---|---|---|---|---|
| 1.0 | 0.8 | no | 1.5 | 25.3 | 78 ± 10 | 40 |
| 2.5 | 0.8 | no | 2.5 | 11.6 | 27 ± 5 | - |
| 5.0 | 1.0 | no | 3.0 | 11.7 | 19 ± 5 | - |
| 10.0 | 1.2 | no | 3.0 | 11.3 | 4 ± 2 | - |
| 2.5 | 0.8 | yes | 2.5 | 21.2 | 20 ± 5 | 23 |
| 5.0 | 1.0 | yes | 1.5 | 27.3 | 20 ± 5 | 3.2 |
| 10.0 | 1.2 | yes | 2.0 | 26.0 | 18 ± 5 | 0.5 |

was calculated according to formula (5). Both calculated and measured efficiencies show that $LN_2$-cooled helium transports recoil atoms with reasonable efficiency up to a distance of 2.5 meters. The difference between the calculated and measured results over longer transport distances can be caused by several factors. First, the validity of the formula used in transmission calculations has not been confirmed at low temperatures. Moreover, the high value of the Reynolds number suggests that the radial flow profile differs from that of a fully developed laminar flow leading to the invalidity of formula (8). Secondly, the presence of impurities in helium ($\lesssim$ 20 ppm ) probably influences the yields to some extent.

In the case of noncooled capillaries, there is heat transfer to a subsonic flow, which results in an additional increase in velocity along the capillary. Because of uncertainties in experimental conditions, the velocity distribution could not be calculated. However, the average time a particle spends in the capillary is shorter than the time given by formula (4). This might be an explanation for the high experimental transport efficiency in the case of one meter capillary.

In order to see if the $LN_2$-cooled system could be used for the transport of charged particles induced recoils, a cyclotron run with $^{60}Cu$ recoils was performed. The recoils were obtained from $^{nat.}Ni$ (p,xn) reactions with 15 MeV protons. The proton current was 100 nA. The 6 m capillary ( i.d. 1.2 mm ) was cooled over its whole length. With pressures of 380 torr and 0.13 torr

in the target and collection chambers and with a flow rate of 47 $cm^3/s$ (STP), the efficiency was about 10 %. This is by a factor of two lower than the experimental values shown in table III.

### 3.3.2. Role of impurities

As described earlier, special attention was paid to the purity of the commercial grade helium. Several kinds of filters were used in order to reduce the original impurity level (20 ppm). No essential differences in transport properties were observed.

The diameter of an impurity cluster leading to a calculated capillary transmission of 18 % in case of a 10 m capillary is 13 Å ( compare table III ). The impurity concentration of 20 ppm corresponds to the cluster concentration of about $3 \times 10^{12}$ clusters/$cm^3$ at the temperature of 80 K and pressure of 2.0 atm. According to simple estimates[32)] the corresponding collision frequency between a given, thermalized, recoil atom and clusters would be about 700 collisions per second, which in favourable conditions can lead to the adhering of a recoil atom onto a cluster. However, one should compare the 20 ppm impurity level to those needed in the carrier-loaded He-jet method. There the minimum concentrations are about one order of magnitude higher.

On the basis of the above-mentioned considerations and the results given in the previous chapter, it appears likely that impurities increase the yields to some extent, especially in the case of long capillaries.

### 3.3.3. Transport of fission products

Fission products differ from alpha-decay recoils in several respects that may influence the transport efficiency: their ranges in helium (STP) extend over several centimeters, their masses are roughly half of those of the alpha-decay recoils, and many more elements with different chemical properties are involved.

In the study of the fission products, the apparatus described in chapter 3.1.3. was used. The capillary was 2.7 m long and 0.8 mm in diameter; it was not cooled. The pressure in the recoil chamber was 3.0 atm. Two X-ray spectra obtained with an 80 $mm^2$ x 3 mm Si(Li) detector are shown in fig. 5. The upper spectrum was recorded from a plastic foil that was placed immediately behind the uranium target during a neutron bombardment. The lower one was measured from a sample that was collected on a catcher foil by means of the helium-jet technique. Collection time was 20 min and measuring time 40 min in each case. The groups were identified on the basis of $K_\alpha$-energies. The similarity of the two curves is striking. In table IV transport efficiencies determined from the spectra are listed for a few chemical elements.

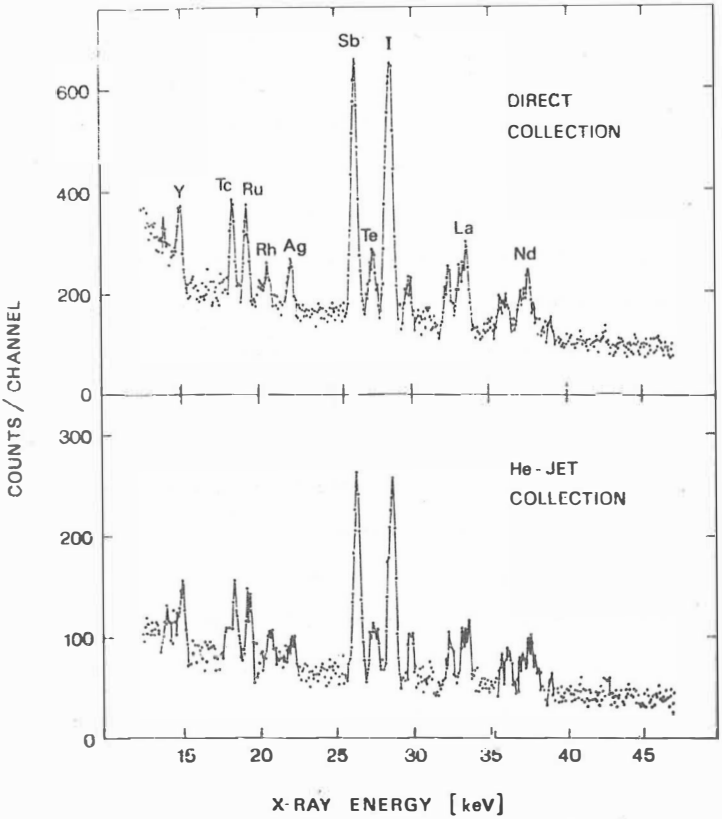


Fig. 5. X-ray spectra obtained from fission products. Direct recoil collection was used in the upper spectrum and the $LN_2$-cooled He-jet transport technique in the lower one.

Table IV. Experimental transport efficiencies for some elements produced by nuclear fission. The efficiencies were determined from the $K_\alpha$-groups of the X-ray spectra shown in fig. 5.

| Element | Efficiency (per cent) |
|---|---|
| Tc | 30 ± 10 |
| Ru | 27 ± 7 |
| Sb | 27 ± 5 |
| I | 24 ± 5 |

These special examples indicate that (1) transport efficiency is largely independent of the chemical nature of the elements, and (2) efficiencies for fission products are roughly equal to those obtained for alpha-decay recoils under similar conditions. These rules appear to be roughly valid for many chemical elements and for a variety of experimental conditions.

# 4. Transport of recoil atoms with carrier-loaded helium

## 4.1. Experimental

In this section the emphasis in the description of the transport apparatus is on the details that are relevant to the use of carriers. The same experimental techniques for recoil production and transport as those described in chapter 3.1. were used.

Several carrier substances were used; some of them were gaseous at room temperature and pressure, others were liquid or solid. The section of the He-jet apparatus that was used for carrier production is shown in figure 6. In the case of gaseous carriers (X), the vaporizer was removed from the line and carrier concentration was regulated by the needle valve in the carrier feed-line. Liquid and solid carriers were introduced into helium by passing it through the vaporizer containing the carrier substance. The vaporizer is simply a chamber with volume of about 50 $cm^3$ placed inside an electrically-heated oven. The temperature of the oven for liquid carriers could be varied from room temperature up to 200°C and for solid carriers from room temperature up to 1000°C. The concentration of carrier substance flowing to the target chamber was controlled by the vaporizer temperature and by the flow rate through the vaporizer. The total flow through the target chamber was kept constant by the second helium line ( fig. 6.).

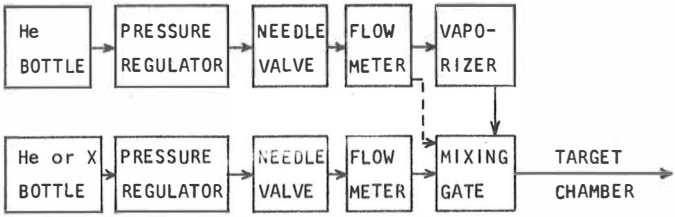


Fig. 6. Schematic diagram showing different steps in the carrier production.

## 4.2. Results

### 4.2.1. Transport efficiencies obtained with different carriers

The necessity for carrier clusters in achieving high transmission yields is fairly well understood on the basis of calculations concerning the internal energetics and diffusion properties of the He-jet. However, there are still many unsolved problems related to the role and the behaviour of the carriers in the transport mechanism. The nature of the carrier clusters, the binding between these and radioactive atoms, the chemical selectivity with respect to the nature of the cluster, the effect of impurities on flow properties

and the expansion of helium and cluster beams from the capillary exit are all matters not well understood.

In this work several carrier substances of different chemical and physical natures were used. Clusters can be produced in several ways. Different kinds of aerosol generators, bubbling chambers, and evaporators have been used[1,13,14,16,17,18]. Even transport gases originally above critical temperature and pressure have been used to generate clusters in the gas itself[14]. In this work, the evaporation technique was used[20].

The formation of clusters is believed to take place in two ways. In the first place, they are formed through condensation and subsequent coagulation of vapor into small droplets when the mixture of helium and vapor flows out of the vaporizer. Secondly, ionic condensation centers, created by the radiation in the target chamber, increase the formation of clusters. This ionization is caused by alpha-particles, fission fragments, recoil atoms from (p,xn) reactions and by the primary charged particle beams passing through the target chamber.

A number of measurements were taken with different gases or vapors mixed with helium. The transport apparatus was used in the standard fashion as described earlier. The concentration of liquid or solid carriers was regulated only by the temperature of the vaporizer, and the second line shown in fig. 6. was not used. The lengths of capillaries were 4.0 or 6.0 m and the diameters 0.6, 0.8 or 1.0 mm. The pressure in the target chamber varied from 1.0 to 3.0 atm and in the collection chamber it was

less than 0.1 torr. The distance of the catcher foil from the capillary exit was 10 mm.

Maximum transport efficiencies obtained in the experiments are listed in table V.

In the case of the $^{227}$Ac-source, acetylene ( $C_2H_2$ ) as a carrier did not bring about any noticeable improvement compared to pure helium. Transport efficiencies with a mixture of propane and butane ( 43 % $C_3H_8$ + 54 % $C_4H_{10}$ ), with carbon tetrachloride ( $CCl_4$ ), and with trichlor-trifluor propane ( $CF_3C(Cl):CCl_2$ ) were roughly an order of magnitude higher. The variation of the efficiency in repeated experiments was large, however, indicating inadequate control of the process. In the case of vacuum pump oil very high transport efficiency was obtained at a relatively low concentration of the carrier. Nearly the same result was obtained for the transport of fission products. The reproducibility of the results with oil vapor was good.

The results for the transport of recoils from the proton-induced reactions differed markedly from those obtained from the $^{227}$Ac-source. This can be seen by comparing the results of the experiments performed with the mixture of propane and butane. The yield was one order of magnitude higher for $^{60}$Cu recoils than for $^{211}$Pb recoils obtained from the $^{227}$Ac-source. A similar trend has also been found in the case of $CCl_4$ as an additive. In this work the transport efficiency was measured to be only 1 %. Schmidt-Ott has measured an

Table V. Maximum transport efficiencies obtained with different carriers. Partial pressures were taken from ref. 20, 33, 34.

| MEANS OF RECOIL PRODUCTION | CARRIER | CAPILLARY L (m) | CAPILLARY Ø (mm) | TARGET CHAMBER PRESSURE (atm) | FLOW RATE (STP) ($cm^3/s$) | VAPORIZER TEMPERATURE (°C) | CARRIER PARTIAL PRESSURE (torr) | EFFICIENCY (%) |
|---|---|---|---|---|---|---|---|---|
| $^{227}Ac$ | $C_2H_2$ | 4 | 0.6 | 2.0 | 17 | gas | 1.5-150 | ≈ 0.1 |
| $^{227}Ac$ | $C_3H_8+C_4H_{10}$ | 4 | 0.6 | 3.0 | 25 | gas | 20 - 30 | ≈ 1 |
| $^{227}Ac$ | $CCl_4$ | 4 | 0.6 | 2.0 | 17 | 20 | 80 | ≈ 1 |
| $^{227}Ac$ | $CF_3C(Cl):CCl_2$ | 4 | 0.6 | 2.0 | 17 | 20-50 | 20-100 | ≈ 0.5 |
| $^{227}Ac$ | OIL | 4 | 0.6 | 2.0 | 17 | 120 | 0.4 | 70 |
| $^{nat.}Ni(p,xn)^{60}Cu$ | $C_3H_8+C_4H_{10}$ | 6 | 1.0 | 1.0 | 25 | gas | 20 - 30 | 10 |
| $^{nat.}Ni(p,xn)^{60}Cu$ | NaCl | 6 | 1.0 | 1.0 | 25 | 750 | 0.1 | 25 |
| $^{nat.}Sn(p,xn)^{116}Sb$ | NaCl | 6 | 0.8 | 1.5 | 24 | 750 | 0.1 | 15 |
| $^{nat.}U(n,f)$ | OIL | 4 | 0.6 | 2.0 | 17 | 120 | 0.4 | 60 |
| $^{252}Cf$ a) | NaCl | 4 | 0.8 | 2.0 | 60 | 750 | 0.1 | 70 |
| $^{252}Cf$ a) | $SnCl_2$ | 4 | 0.8 | 2.0 | 60 | 280 | 0.3 | 40 |

a) target chamber cooled with liquid nitrogen

efficiency of 48 % for Dy recoils obtained from the reaction $^{141}Pr\ (^{14}N,\ 5n)^{150}Dy$ [35].

The use of solid particles as carriers was also tested. In cases of NaCl and $SnCl_2$ high transport yields were observed. It should be noted that, in experiments with fission products from the $^{252}Cf$-source, the source chamber was cooled with liquid nitrogen

On the basis of the above results the hypothesis of two-fold cluster formation process seems to be justified. Some of the carriers can condense into stable droplets even before arriving in the target chamber, being typically liquids and solids that have very small vapor pressures at the temperature at which the He-jet apparatus is operated. On the other hand, especially in the case of $CCl_4$ and $C_3H_8 + C_4H_{10}$ , the intensity of the ionizing radiation seems to have an effect on the cluster formation and consequently on the transport efficiency.

4.2.2. Concentration of the carrier

The amount of carrier substance in the transport gas depends on the vapor pressure of the carrier and on the flow rate of helium through the vaporizer. In general, the pressure of a saturated vapor depends on the temperature according to the relation $^{10}\log p = A - B/T$, where p is the saturated vapor pressure (torr), T is the absolute temperature (K) and A and B are constants[27]. Figure 7. shows this dependence graphically for the vapors that were used in this work[20,33,34]. The curve for NaCl is not shown in the figure. It has a vapor pressure of $3.0 \times 10^{-2}$ torr at 700°C and $3.8 \times 10^{-1}$ torr at 800°C [34].

On the basis of the curves, it is evident that acetylene ($C_2H_2$) and propane ($C_3H_8$) cannot form droplets in the transport system when operated at room temperature. For other compounds, condensation is possible before arrival in the target chamber. Table V shows that the higher the vapor pressure is the larger amount of carrier substance is needed for efficient transport. In cases of vacuum pump oil, NaCl and $SnCl_2$ the partial pressure of the carrier is of the order of 0.1 torr, which is two orders of magnitude lower than the partial pressures of the other substances used. Because of the problems caused by the high vapor pressure when coupling the He-jet method to the ion source of the isotope separator, the subsequent studies were performed

with carriers having low vapor pressure and thus low concentration.

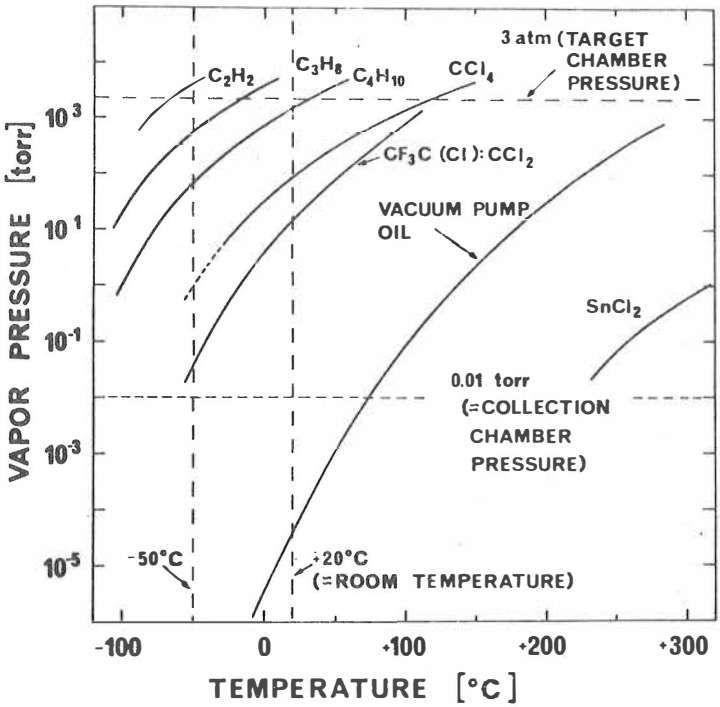


Fig. 7. Vapor pressure as a function of temperature for different carriers that were used in this work.

Within wide limits transport efficiency does not depend noticeably on the target chamber pressure when carrier-loaded helium is used. Instead it turns out to be highly sensitive to changes in the concentration of the carrier. The optimum condition is a balance between insuring adequate cluster formation and keeping the system clean.

A number of experiments were performed to determine the optimum carrier concentration for proper operation of the transport system. Vacuum pump oil and NaCl were used as carriers in these experiments. Two examples of the measurements obtained are shown in figure 8. In these measurements the concentration of the carrier vapor in the helium was regulated only by the temperature of the vaporizer and the second line shown in fig. 6. was not used. The flow parameters were the same as those given in table V.

The steep rise of the curves at lower temperatures can be understood in terms of the rapid change of the saturated vapor pressure with increasing temperature ( see fig. 7.). When a certain concentration of the carrier is reached, practically all produced recoils are adsorbed by the clusters and the curves level-off. Comparison of the two curves shows that recoils from the Ni(p,xn)-reaction are transported with a considerably lower efficiency than recoils from the $^{227}$Ac-source. The difference is possibly due to the small ranges of recoils ($\approx$ 1 mm) from proton induced reactions, and low cluster concentration near the target surface. Alpha-decay recoils

are produced via the decay of the gaseous $^{219}Rn$ and can reach the higher concentration area in the target chamber.

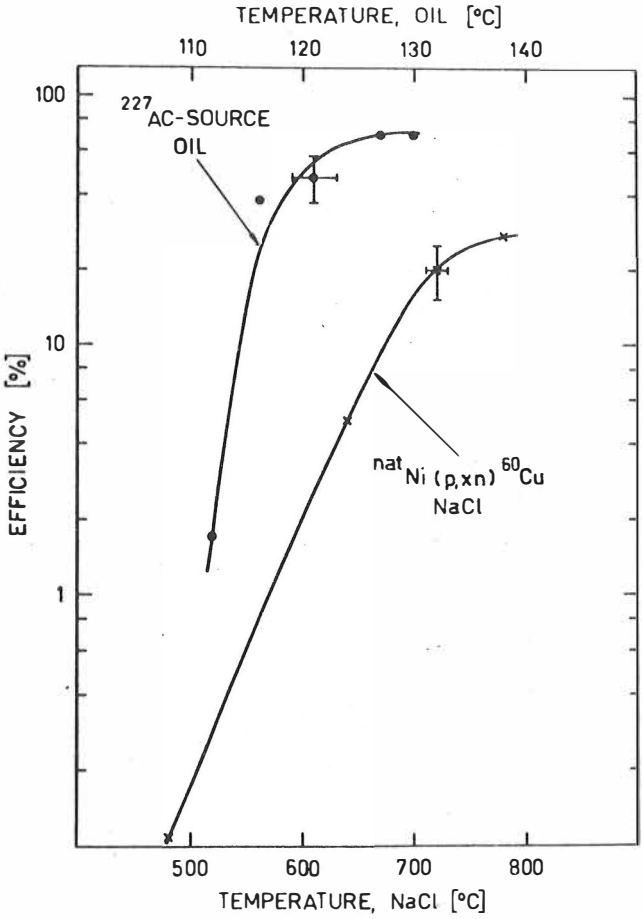


Fig. 8. Transport efficiency as a function of temperature of the vaporizer. The curves are not fitted through the experimental points.

The calculated mass flow of carrier vapor from the vaporizer was 0.1 mg/s in the case of oil, at the temperature of 127°C. The corresponding value for NaCl was 0.01 mg/s at the temperature of 750°C. On the other hand, the amount of carrier substance adsorbed on the catcher foil during the run was typically by a factor of five smaller than the value obtained from the mass flow of vapor. Thus, a considerable amount is adsorbed in the transport system. Transmission calculations, to be presented in the following chapter, show that the main area of loss is the line between the vaporizer and the target chamber.

### 4.2.3. Size of carrier particles

Typically, the diameters of clusters produced by evaporation extend from $10^{-3}$ µm up to diameters of 0.1 µm [36]. During transportation into the target chamber, the cluster size distribution is further affected by the growth of particles by coagulation into and out of various size ranges[28,36]. The size range of clusters entering the target chamber is finally determined by the transmission properties of the line connecting the vaporizer to the target chamber. The calculated transmission for two different systems, which are at present used to transport activities into the ion source of the isotope

separator, are shown in fig. 9. Calculations were performed with the formulae given in capters 2.2.1. and 2.2.2., assuming a parabolic flow profile. The density of a NaCl cluster was taken to be 2.16 g/cm$^3$ [33].

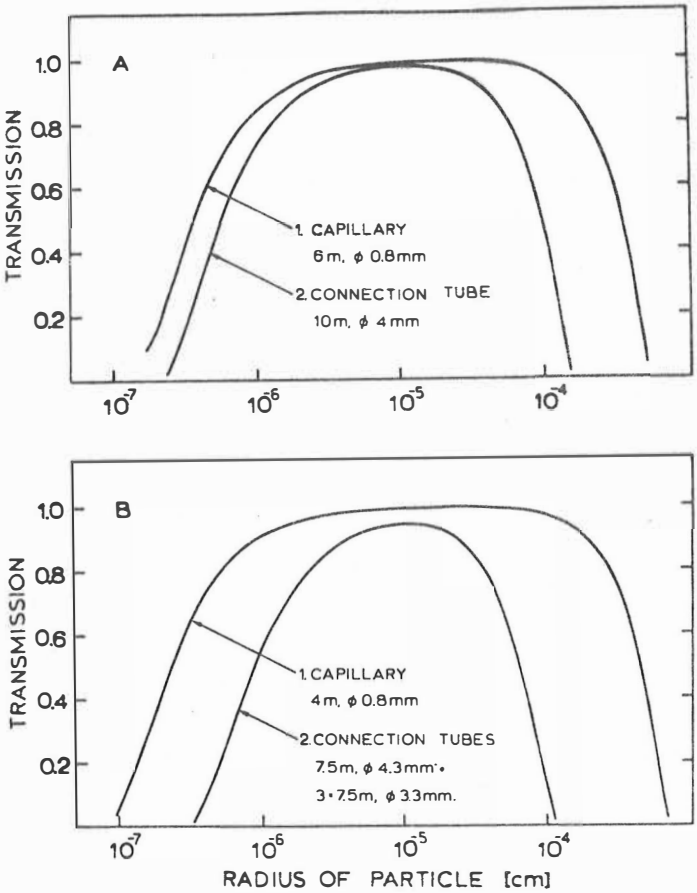


Fig. 9. Calculated transmission of NaCl clusters through the He-jet system. Target chamber pressures: A 1.5 atm, B 2.0 atm. A detailed description of the figure is given in the text.

The upper curves represent the transmission for the apparatus used to transport recoils from the target chamber placed in the cyclotron beam line. The tube connecting the vaporizer and the target chamber has a length of 10 m and a diameter of 4 mm. A comparison of the two curves shows that clusters which enter the target chamber and have a radius greater than $10^{-4}$ cm ( = 1 μm ) are transported with very small losses through the capillary. In the size range below $10^{-6}$ cm ( 0.01 μm ) the two curves are close to each other and considerable losses are predicted in the capillary.

The lower curves represent the transmission for the apparatus used to transport fission products from the $^{252}$Cf-source. In this case the transport line from the vaporizer to the Cf-chamber is composed of a tube, having a length of 7.5 m and a diameter of 4.3 mm, coupled to three parallel tubes with a length of 7.5 m and a diameter of 3.3 mm each. The width of the transmission curve through the connection tubes is considerably smaller than that of the capillary. This results in small losses in the capillary both in the case of small and large clusters.

Using the present method of cluster production, the exact regulation of the sizes as well as of the concentration of clusters is not possible. However, the line between the cluster generator and the target chamber can be used as a filter to remove those sizes that are not well transported through the capillary. On the other hand, the cluster concentration can be affected by changing both the temperature and the helium flow rate in the vaporizer.

In order to get an idea of the cluster size distribution, a series of measurements were taken with fission products from the $^{252}$Cf-source by changing the temperature and the flow rate in the vaporizer. The pressure in the source chamber was kept at 2 atm and the total flow through the system was 39.2 $cm^3/s$ (STP). Fission products were collected on a moving tape, and gross β-activity was continuously monitored by a plastic scintillator. The transported activity was measured as a function of the flow rate through the vaporizer at several temperatures. It was observed that the yield increased rapidly at a certain flow rate to a maximum value and remained essentially constant up to the maximum flow rate used. The results are summarized in table VI. The second column gives the minimum fraction of the flow through the vaporizer ( $= Q_2/Q_{TOT}$ ) corresponding to the maximum yield given in the last column. The third and fourth columns give the calculated minimum and maximum mass flows of NaCl between which the yield stayed constant. It is interesting to note that the yield starts to decrease at temperatures above 800°C. It is obvious that, at high concentrations, coagulation effects give rise to an increase in average cluster size. Clusters having a size well above 1 μm will not be transported to the target chamber. Consequently the cluster concentration will decrease giving rise to a decrease in the transport yield through the capillary. The amount of NaCl adsorbed on the catcher was found to follow the behaviour of the yield, confirming the decrease in the concentration at high temperatures.

Table VI. Dependence of transport yield on mass flow of NaCl.

| Temperature (°C) | $Q_2/Q_{TOT}$ (minimum) | Mass flow of NaCl min. (μg/s) | max. (μg/s) | Relative yield |
|---|---|---|---|---|
| 600 | - | - | 0.07 | 0.04 |
| 650 | 0.7 | 0.3 | 0.5 | 0.67 |
| 710 | 0.5 | 1.4 | 2.8 | 0.93 |
| 750 | 0.5 | 3.9 | 7.8 | 1.00 |
| 800 | 0.4 | 10.4 | 26.1 | 0.96 |
| 840 | 0.3 | 17.0 | 56.5 | 0.70 |

The reduction of the carrier mass flow by the method of flow fractioning is of great practical importance in the coupling of the carrier loaded He-jet to the ion source of the isotope separator. The minimum mass flow of NaCl from the vaporizer at the temperature of 750°C was 3.9 μg/s, corresponding to the concentration of about 500 ppm ( in weight ) and 30 ppm ( in volume ). If the average cluster size were 0.1 μm and there were no losses in transport to the target chamber, the concentration of NaCl clusters

( $\rho$ = 2.16 g/cm$^3$ ) in the target chamber would be 2.4 x $10^7$ clusters/cm$^3$. If the radius were 0.5 µm, the corresponding concentration would be 1.9 x $10^5$ clusters/cm$^3$. These numbers are of the same order of magnitude as those given by Wiesehahn[14].

### 4.2.4. Chemical selectivity

In general, the transport mechanism does not appear to be selective with respect to chemical elements. This argument has been verified by the use of a variety of cluster materials and reactions throughout this study. Results seem to indicate that the interaction between thermalized recoils and clusters is something like physical adsorption due to Van der Waals-type bindings.

This is supported by the successful radiochemical separations made for samples that were collected by the He-jet method[4]. In the experiments where the radioactivity was brought into a liquid phase, $^{211}$Bi was separated from $^{211}$Pb by means of a dithizone extraction[4]. The separation yield was almost 100 %. Extraction was also used for radiochemical separation of fission products. The mixture of propane and butane, $CF_3C(Cl):CCl_2$, and vacuum pump oil were used as carriers in these experiments. With a strong chemical binding between the active atoms and the carrier molecules these separations would not have been possible.

## 5. On-line isotope separation employing the He-jet technique

### 5.1. General

In most on-line separator systems, the primary beam from the accelerator passes through a target that is placed in the ion source of the separator[22,23,24]. Because of their kinetic energies, the recoil atoms to be separated are buried in the walls of the ion source. They are partly returned to the plasma by thermal diffusion but time delay and loss of intensity cannot be avoided. This type of technique is inherently applicable only to volatile nuclides and their daughter activities. Another way to perform on-line mass separation is to produce radioactive atoms outside the ion source and transport them into the source by means of diffusion or gas flow. The diffusion technique is applicable only in the case of highly volatile elements and requires very high temperatures and complicated technical constructions[22,23,24]. The transport of activities into the ion source using helium gas as a transporting medium is a promising alternative to the methods mentioned above[7-11]. In general, the He-jet method is not selective with respect to chemical elements; nonvolatile elements can be brought into the ion source as easily as volatile ones. The choice of the ion source and the design of the delicate coupling of the He-jet to

it then become major factors that determine the efficiency of the entire system.

The use of helium rather than some other transport gas has several advantages. Its chemical inactivity, its resistance to nuclear reactions and its high ionization potential are all factors which favor the use of helium. The high ionization potential allows high flow rates into the separator vacuum system without difficulties as far as voltage breakdowns are concerned. The choice of carrier substance has great practical importance. In this work, NaCl was used as carrier in experiments with the isotope separator. Organic carrier substances were thought to cause difficulties in the operation of the ion source and also to lead to inter-contamination between adjacent masses in the mass separation. Moreover, the low vapor pressure of NaCl even at high temperatures is important in minimizing the effect of temperature on cluster dissociation and thus on divergence of the beam of clusters entering the skimmer/ion source system. The high-voltage stability of the separator is also improved compared to the situation with carriers with high vapor pressure.

The system used in this work consists of a target chamber mounted in the external beam line of a 90 cm cyclotron; an ISOLDE I-type isotope separator; and a flexible He-jet system that connects the target chamber to the separator ion source. When desired, the target chamber can be replaced by the $^{252}$Cf or $^{227}$Ac-source. Two different combinations of helium-jet and ion source were investigated: one employing a pure helium-jet

at liquid nitrogen temperature connected to a Nielsen type ion source, and the other employing a NaCl-loaded helium-jet in combination with a hollow cathode ion source.

## 5.2. Experimental

### 5.2.1. He-jet apparatus.

Both the liquid nitrogen-cooled and NaCl-loaded He-jet techniques were used. The experimental apparatus was the same as described in chapters 3.1. and 4.1. The efficiency of the system was measured off-line by alpha-, beta-, X-ray and gamma counting.

The coupling of the transport capillary to the isotope separator is shown in fig. 10. The gas jet expanding from the capillary is directed into the ion source through two consecutive skimmers. The skimmers remove the bulk of helium, but let heavy clusters pass through. The skimmer chamber is evacuated with a Roots blower, and the space between the two skimmers with a diffusion pump. The acceleration chamber of the separator is evacuated by a separate diffusion pump.

The skimmer chamber is at the high potential ( 60 kV ) of the ion source while the target chamber and the Roots blower are at ground potential. To prevent electrical discharges,

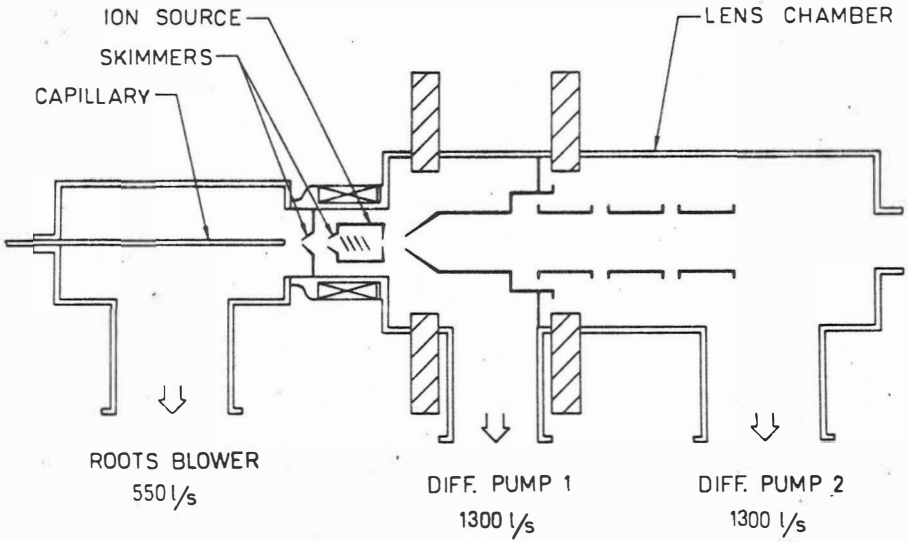


Fig. 10. Diagram of the differential pumping system.

a voltage divider consisting of a series of metal-net electrodes was built inside the PVC-plastic tube, 3 m long and 20 cm in diameter, that connects the skimmer chamber and the blower. The total resistance of the line is 340 MΩ corresponding to "dark" current of 150 μA, when the ion source is run at 50 kV potential. This current corresponds to about 30 % of the capacity of the present high voltage power supply. The maximum helium pressure that can be maintained in the skimmer chamber without a voltage breakdown is about 0.15 torr. The connection line reduces the pumping speed by a factor of two.

### 5.2.2. Coupling of the cooled He-jet to the Nielsen ion source

The width of the angle into which the transported radioactive atoms spread at the capillary exit is an important factor in the choice of the ion source and in the design of the skimmer/ion source geometry. The average angle of divergence for $^{211}$Pb recoils was measured to be 11 ± 2$^{o}$ for cooled helium[20]. At room temperature the angle of divergence for atoms of mass number A = 220 has been measured to be 30$^{o}$ [1].

The standard Nielsen type ion source[37] with its large volume ( 31 cm$^{3}$ ) and inner diameter ( 2.7 cm ) allows a wide angle of divergence and was therefore chosen for use with a cooled helium-jet. The ion source and its coupling to the He-jet capillary is shown in fig. 11. The choice of the skimmer diameters is determined by the angle of divergence of activities and by the pumping capacity of the system. On the other hand,

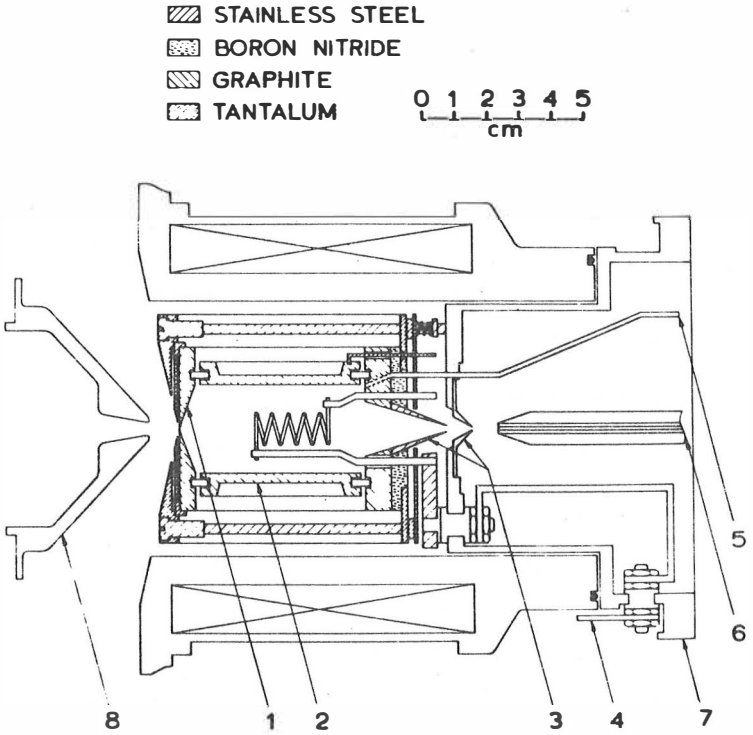


Fig. 11. The modified Nielsen ion source and its coupling to the He-jet capillary. Key to the reference numbers: 1. end plate (anode potential), 2. anode cylinder, 3. skimmers, 4. current feed for filament, 5. gas feed, 6. capillary, 7. wall of the skimmer chamber, 8. extraction electrode.

the mass throughput of helium should be high in order to achieve efficient transport through the capillary. The first and second skimmers have hole diameters of 1.25 mm and 2.0 mm, respectively. The distance from the end of the capillary to the first skimmer is 8 mm corresponding to an acceptance angle of about $9^{o}$. The flow rate of helium through the capillary was typically 50 $cm^3/s$, corresponding to a pressure of 0.14 torr in the skimmer chamber. Pressures, measured at the pump inlets, in the ion source region, and in the lens chamber, were $8 \times 10^{-5}$ torr and $10^{-6}$ torr.

In order to achieve higher temperatures, the end plate and the anode cylinder of the ion source were connected to the same potential. The extraction hole was 1.5 mm in diameter. Xe was used as a support gas and as a mass marker when possible. The pressure inside the source was estimated to be about $10^{-2}$ torr. Characteristic values for ion source operation were: anode current 1.5 A, anode voltage 60 V, filament current 36 A and filament voltage 7 V. Typically, the extraction electrode to ion source distance was 10 mm and the extraction voltage 17 kV. With these parameters, an Xe current of 50 μA and an He current of several μA were obtained. In these conditions the mass resolving power was about 200. The lifetime of the ion source or the filament is of practical importance in the operation of the source. The Nielsen source, with parameters given above, could be operated for several days without a breakdown.

### 5.2.3. Coupling of the NaCl-loaded He-jet to the hollow cathode ion source

The carrier loaded He-jet coupled to an ion source has some important advantages over the cooled He-jet. Two of these are the high transport effciency with long capillaries and the small angle of divergence of the heavy clusters. The latter allows the use of small-volume ion sources like the different versions of the hollow cathode sources described by Sidenius[38,39].

Several versions of the hollow cathode source, with both cathode and anode extraction, were tested. The latest and the most promising version is presented in fig. 12. The diameter of the extraction hole was 0.5 mm and that of the plasma expansion cup 1.5 mm. A larger extraction hole caused instabilities. The diameter of the plasma column between the filament and the anode was varied. Experiments with the pair of fission products $^{141}Cs \rightarrow {}^{141}Ba$ showed that equal efficiencies were obtained with diameters of 7 mm and 4 mm. The 4 mm column was used in subsequent studies because of higher arc current density and hence better heating of the anode.

Support and mass marker gases were fed directly into the plasma region. This was done to minimize gas flow into the ion source and hence to minimize the pressure in the extraction region. With the carrier loaded He-jet method, the flow rate of helium and the divergence of the cluster beam containing the activities are considerably smaller than with the cooled

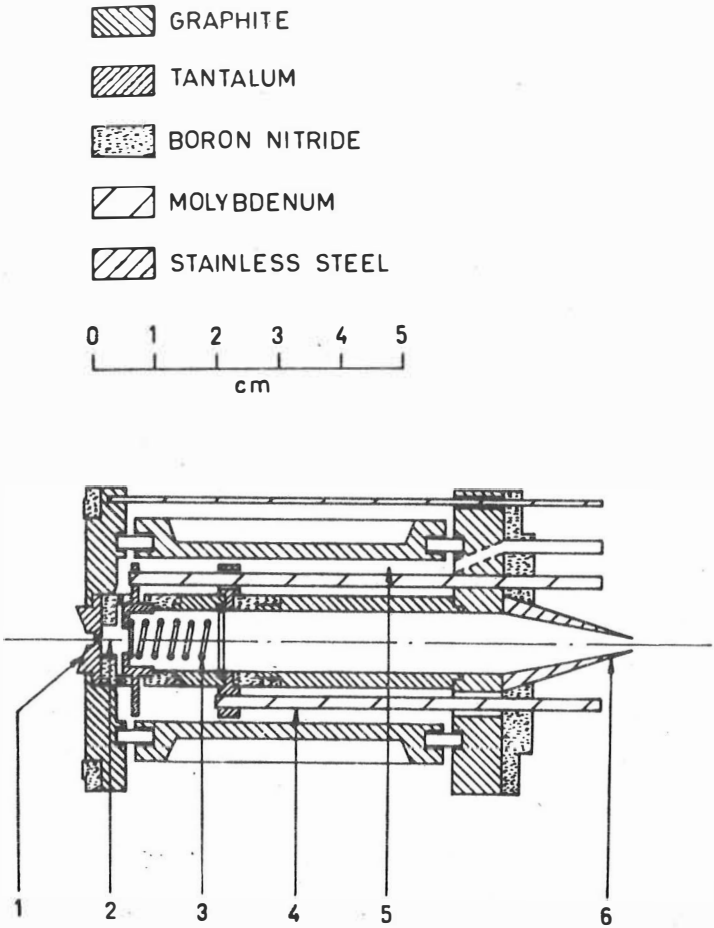


Fig. 12. The modified hollow cathode ion source. Key to the reference numbers: 1. anode plate, 2. plasma region, 3. filament, 4. current feed for filament, 5. gas feed channel, 6. second skimmer.

system. This allows the use of skimmers with smaller diameters which can be placed closer to the capillary exit. In the present version, the skimmer diameters were 1.0 mm and 2.0 mm. The capillary to skimmer distance was 5 mm which corresponds to an upper limit of about $11^{o}$ for the angle of divergence. The angle of divergence for NaCl clusters which had traversed the first skimmer was measured and found to be $7^{o}$ ( FWTM = full width at tenth maximum ). The corresponding angle without a skimmer was $8^{o}$ (FWTM) and $5^{o}$ (FWHM). The diameter of the ion source cylinder at the position of the filament was 9 mm, corresponding to an angle of $8^{o}$ from the capillary.

With a typical flow rate of 20 $cm^3/s$ (STP), the pressure in the skimmer chamber was 0.06 torr. The pressure at the inlets of the first and second diffusion pumps were $7 \times 10^{-5}$ torr and $10^{-6}$ torr, respectively.

Characteristic values for the ion source parameters were as follows:

| | | |
|---|---|---|
| anode current | 2.5 | A |
| anode voltage | 90 | V |
| filament current | 30 | A |
| filament voltage | 12 | V |
| magnetic field | 300 | gauss. |

Xe was used as a support gas. Typical Xe and He currents were 50 µA and 25 µA. The current corresponding to the mass of an NaCl molecule was about 20 µA. These values correspond to the extraction electrode distance of 10 mm and the extraction voltage of 15 kV. The mass resolving power was about 400 for $^{136}Xe$. The lifetime of the filament was 10-15 hours. This should be compared with the long lifetime of the Nielsen source operated with pure helium.

## 5.3. Results with the $LN_2$-cooled He-jet

The total efficiency of the separator was studied by means of proton induced reactions. In addition, runs were performed with both the $^{227}Ac$ and $^{252}Cf$ sources.

The results of the efficiency measurements for separation on-line are summarized in table VII. The He-jet transport efficiencies of 20 % and 30 % were measured for recoil atoms from $^{227}Ac$ and $^{252}Cf$ sources when a transport distance of 3 m was used. In these cases the capillary ( i.d. 0.8 mm ) was not cooled. The corresponding efficiency for $^{60}Cu$ recoils was 10 % when a cooled, 6 m capillary ( i.d. 1.2 mm ) was used. The details are given in chapter 3.

The transmission through the skimmers was measured by gross beta-activity of fission products. It was found to be 25 % through the first skimmer and 50 % through the second skimmer. According to how far the angle of divergence depends on the particle mass, higher transmission is expected for heavier particles. This effect probably explains the high skimmer/ion source efficiency for $^{211}Pb$ ( see table VII ).

The efficiency of the ion source for a certain chemical element is closely related to the volatility of that element. For example, the vapor pressure of copper reaches $10^{-2}$ torr, the estimated pressure inside the ion source, at 1273°C. This temperature is considerably higher than that of the ion source, and consequently a poor ion source efficiency is observed.

Table VII. Efficiencies obtained with the liquid nitrogen cooled He-jet coupled to the Nielsen source.

| MEANS OF PRODUCTION | PRODUCT NUCLIDE | EFFICIENCY (%) | | |
|---|---|---|---|---|
| | | He-JET | SKIMMER ION SOURCE[c)] | TOTAL |
| Ni(p,xn) | $^{60}Cu$ | 10[a)] | < 0.1 | < 0.01 |
| Cu(p,xn) | $^{63}Zn$ | ≈10[a)] | ≈ 0.3 | 0.03 |
| Cd(p,xn) | $^{112m}In$ | ≈10[a)] | ≈ 1.2 | 0.12 |
| Sn(p,xn) | $^{116}Sb$ | ≈10[a)] | ≈ 0.3 | 0.03 |
| $^{252}Cf$ | $^{141}Cs$, $^{141}Ba$ | 30[b)] | 0.3 | 0.1 |
| $^{227}Ac$ | $^{211}Pb$ | 20[b)] | 1.5 | 0.3 |

a) capillary length 6 m

b) capillary length 3 m

c) based on the observed He-jet and total efficiencies

It is interesting to note that, after separation, nearly 100 % of the activity found inside the ion source was concentrated within a radius of 0.5 cm around the exit hole of the ion source. The spot size corresponds roughly to the beam size at that distance from the capillary exit.

When the Nielsen source was operated without direct arc in the oscillating electron mode, the efficiency was one order of magnitude below the values shown in table VII.

## 5.4. Results with the NaCl-loaded He-jet

### 5.4.1. Efficiency measurements

Results of the efficiency measurements with the hollow cathode source are given in table VIII.

Table VIII. Efficiencies obtained with the NaCl-loaded He-jet coupled to the hollow cathode ion source.

| MEANS OF PRODUCTION | PRODUCT NUCLIDE | EFFICIENCY (%) | | |
|---|---|---|---|---|
| | | He-JET | SKIMMER ION SOURCE[c)] | TOTAL |
| Ni(p,xn) | $^{60}Cu$ | 25[a)] | 1.2 | 0.3 |
| Cd(p,xn) | $^{112m}In$ | 15[a)] | 1.7 | 0.25 |
| Sn(p,xn) | $^{116}Sb$ | 15[a)] | 1.3 | 0.2 |
| $^{252}Cf$ | $^{141}Cs$, $^{141}Ba$ | 70[b)] | 1.4 | 1.0 |

a) capillary length 6 m
b) capillary length 3 m
c) based on the observed He-jet and total efficiencies

In the case of $^{141}Cs \rightarrow {}^{141}Ba$, a 4 m capillary (i.d. 0.7 mm) was used. The He pressure was 1.7 atm and the pressure in the skimmer chamber 0.04 torr. The target chamber was cooled with $LN_2$. The (p,xn) reaction products were studied using a 6 m capillary (i.d. 0.8 mm). The target and skimmer chamber pressures were 1.5 atm and 0.06 torr. The NaCl vaporizer temperature was typically between 750°C and 800°C. For details of the He-jet system see chapter 4.

In optimum conditions, a total efficiency of about 1 % was achieved ( see table VIII ). The skimmer transmission for the carrier loaded He-jet is typically about 50 % [8]. Assuming this to be the case, ionization efficiencies of 2.4 % for Cu and 3.4 % for In are obtained. The values should be compared with the results obtained with $LN_2$-cooled pure helium coupled to the Nielsen source, for which estimated ionization efficiencies are < 1 % for Cu and 10 % for In. It should be noted that in the derivation of the skimmer/ion source efficiency, the separator transmission was assumed to be 100 %. In general, efficiencies obtained during this study are comparable to those measured by other groups[8,11].

A somewhat smaller skimmer transmission was observed in the experiments with the cyclotron than with the $^{252}Cf$-source. The larger angle of divergence of clusters in experiments with the cyclotron is probably due to the 90° bending of the capillary before the end and to the presence of small size clusters ( see the upper curve in fig. 9 on page 47). It has been found that

the spatial distribution of clusters emerging from the capillary is strongly dependent on the secondary flow induced by capillary bends upstream[18]. In experiments with the $^{252}$Cf-source the capillary was straight for the last 3 m and the presence of small size clusters was prevented by the poor transmission of the tube connecting the vaporizer and the $^{252}$Cf chamber ( see the lower curve in fig. 9 on page 47).

### 5.4.2. Separation of proton induced fission products

The NaCl-loaded He-jet coupled to the hollow cathode ion source was applied to the separation of fission products from the $^{nat.}$U(p,f) reaction. The target assembly shown in fig. 3 (p. 23 ) was operated at room temperature. Two uranium foils (thickness 45 mg/cm$^3$) were placed close to the windows. The He pressure in the target chamber was 2 atm and the temperature of the vaporizer was 800$^{\circ}$C. Two gamma ray spectra from fission products corresponding to masses 130 - 131 and 141 are shown in fig. 13. Spectra were measured with a coaxial 40 cm$^3$ Ge(Li) detector. Both the collection and measurement time were 15 minutes. The time from the end of the collection to the start of the measurement was 2 minutes.

The preliminary results show that the present combination does not apply to the separation of highly nonvolatile elements.

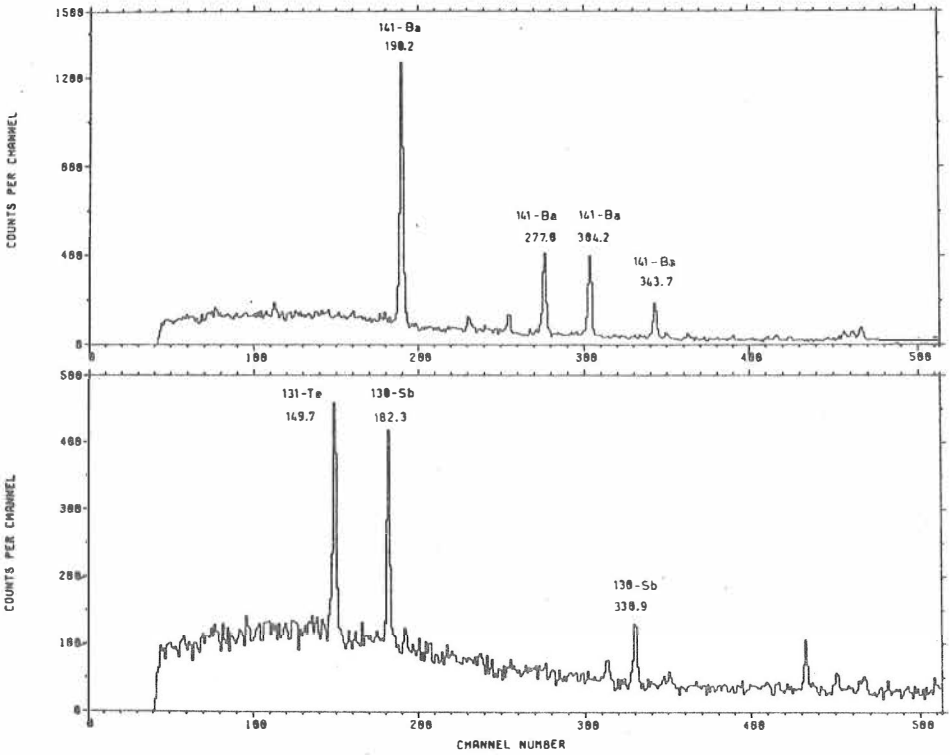


Fig. 13. Gamma ray spectra of fission products corresponding to masses 141 and 130 - 131. Energies are taken from refs. 40, 41 and 42.

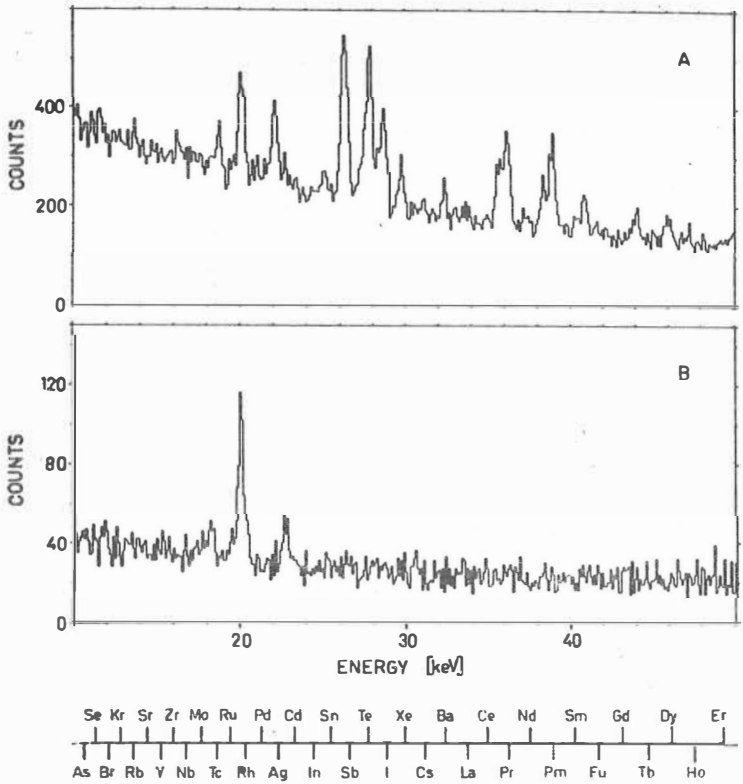


Fig. 14. Low energy spectra of fission products measured from the ion source after a half an hour run. Spectrum A: measured from the cylinder behind the skimmer. spectrum B: measured from the anode plate. Elements shown are ranked according to their $K_{\alpha 1}$ energies.

Experiments with transition elements from Y to Pd resulted in a poor total transmission. In order to study the ion source temperature, a half an hour run was made and low energy spectra from the end plate and the inlet cylinder of the ion source ( see fig. 12 ) were measured 4 hours after the end of the run. In this measurement an ORTEC LEPS detector was used. Spectra are shown in figure 14. In the lower part of the figure, relevant elements are ranked according to their $K_\alpha$ X-ray energies. On the basis of the two spectra, it is evident that a higher ion source temperature is necessary for efficient separation of light mass, highly nonvolatile fission products. The absence of K-X-ray lines for lanthanides in the lower spectrum indicates that the temperature of the end plate is well above 1500°C. In spite of the absence of these elements, their separation yields were considerably smaller than the yield for $^{141}Cs \rightarrow {}^{141}Ba$.

## 6. Discussion

The results presented in previous chapters show that high transport efficiencies with long transport distances can be achieved by cooling helium down to liquid nitrogen temperature or by loading helium with a suitable carrier substance. Pure helium at room temperature was found to transport radioactivities effectively only over a distance of a few centimeters. Theoretically calculated capillary transmissions agreed rather well with experimental results. These calculations have a great practical importance in the design of the transport systems for different applications. For example, the cluster size distribution in the carrier-loaded He-jet method can be selectively controlled by proper design of the line connecting the vaporizer and the target chamber. The minimization of the carrier concentration is important in cases where thin sources are desirable. A small concentration also leads to less activity caused by the carrier substance itself. The condition of minimum carrier concentration is best achieved by using a carrier substance that has a low vapor pressure at the temperature at which the He-jet is operated. In this work NaCl was found to meet the above requirements best. In cases where no carriers can be tolerated, as in some applications of particle spectroscopy, $LN_2$-cooled He-jet should be used. The use of $LN_2$-cooled pure helium also

totally eliminates problems of carrier activation.

The results given in this work indicate that the NaCl-loaded He-jet system coupled to the hollow cathode type ion source has several advantages over the $LN_2$-cooled He-jet coupled to the Nielsen source. Among these are a better performance for elements with a high melting point and a higher overall efficiency. However, for low melting point elements, the ionization efficiency of the Nielsen source was equal or even better (In) than that of the hollow cathode source. The $LN_2$-cooled pure helium-jet system was also tested coupled to the hollow cathode source. The total efficiency measured for $^{116}Sb$ was about the same as it was with the Nielsen source. Conversely, the yield obtained with the Nielsen source coupled to the NaCl-loaded He-jet gave an efficiency of about a half of that obtained with the hollow cathode source.

The lifetime of the ion source or the filament is of practical importance in the operation of the ion source. The Nielsen source coupled to pure He-jet could be operated for several days without a breakdown, while the lifetime of the hollow cathode source with NaCl-loaded helium was only 10 - 15 hours. The lifetime of a source can probably be lengthened by the use of smaller anode voltages and by shielding the filament from direct bombardment of the incoming NaCl beam.

The outer parts of the hollow cathode source should be

modified for better performance. In the present version the source has too large a heat capacity and a complicated structure. By increasing the cooling power and by making the structure lighter outgassing problems and severe heating-up of the whole ion source region could be avoided. Moreover, the geometry of the extraction electrode and the shape of the magnetic field in the extraction region should be optimized in order to get more intense beams with better mass resolving power.

The present hollow cathode source used in connection with the NaCl-loaded He-jet cannot be used for the separation of highly nonvolatile elements like those in the lower mass peak of fission products. A solution to this problem could be the use of different chlorides or other chemically reactive substances as carriers instead of NaCl, in order to get elements as compounds with higher volatility into the ion source.

In the near future there will be a strong emphasis on the use of both the He-jet method and the on-line isotope separator in the study of nuclear structure. The He-jet apparatus described in this work has already been successfully used to investigate short lived isomeric states ($T_{1/2} \approx 0.1$-1 s) in Au isotopes[43] and delayed-particle emission of some light nuclei[44]. In parallel with these applications, special attention will be paid to the reduction of the total transport time and to the development of measuring techniques at the

collection site. The isotope separator will further be developed, and it will be devoted to studies of decay properties of short lived fission products, especially of those that are nonvolatile and are difficult to separate using other existing methods.

References

1. R.D. Macfarlane, Nuclear Spectroscopy, vol. II, ed. J. Cerny; Academic Press, New York, 1972

2. A. Ghiorso, M. Nurmia, J. Harris, K. Eskola, P. Eskola, Phys. Rev. Lett. 22 (1969) 1317

3. K. Valli and E.K. Hyde, Phys. Rev. 176 (1968) 1377

4. P. Puumalainen, J. Äystö and K. Valli, Nucl. Instr. Meth. 112 (1973) 485

5. K.L. Kosanke, Wm.C. Mcharris and R.A. Warner, Nucl. Instr. Meth. 115 (1974) 151

6. K. Hellmuth and K. Valli, Nucl. Instr. Meth. 125 (1975) 99

7. J.P. Zirnheld, Nucl. Instr. Meth. 114 (1974) 517

8. W.-D. Scmidt-Ott, R.L. Mlekodaj, E.H. Spejewski and H.K. Carter, Nucl. Instr. Meth. 124 (1975) 83

9. R.A. Gough, J. Cerny, D. Moltz, M.S. Zisman and D.J. Vieira, Symposium on Target Techniques for On-Line Separators, Aarhus, Denmark, September 4-5,, 1975

10. J. Äystö, V. Rantala, K. Valli, S. Hillebrand, M. Kortelahti, K. Eskola and T. Raunemaa, Nucl. Instr. Meth. 139 (1976) 325

11. A.K. Mazumdar, H. Wagner, W. Walcher and T. Lund, Nucl. Instr. Meth. 139 (1976) 319

12. W.-D. Schmidt-Ott, in symp. given in ref. 9

13. A. Ghiorso, J.M. Nitschke, A.R. Alonso, G.T. Alonso, M. Nurmia, G.T. Seaborg, E.K. Hulet and R.W. Lougheed, Phys. Rev. Lett. 33 (1974) 1490

14. W.J. Wiesehahn, G. Bischoff and J.M. D'Auria, Nucl. Instr. Meth. 124 (1975) 221

15. C. Weiffenbach, S.C. Gujrathi, J.K.P. Lee and A. Houdayer, Nucl. Instr. Meth. 125 (1975) 245

16. H. Wollnik, H.G. Wilhelm, G. Röbig and H. Jungclas, Nucl. Instr. Meth. 127 (1975) 539

17. H. Schmeing, V. Koslowsky, M. Wightman, J.C. Hardy, J.A. MacDonald, T. Faestermann, H.R. Andrews, J.S. Geiger and R.L. Graham, Nucl. Instr. Meth. 139 (1976) 335

18. W.J. Hiller and W.-D. Schmidt-Ott, Nucl. Instr. Meth. 139 (1976) 331

19. J. Äystö and K. Valli, Nucl. Instr. Meth. 111 (1973) 531

20. J. Äystö, P. Puumalainen and K. Valli, Nucl. Instr. Meth. 115 (1974) 65

21. J. Äystö, S. Hillebrand, K. Hellmuth and K. Valli, Nucl. Instr. Meth. 120 (1974) 163

22. In Proc. the 8th Int. EMIS Conference, Skövde, Sweden, June 12-15., 1973

23. In Symp. on Target Techniques for On-Line Separators, Aarhus, Denmark, September 4-5., 1975

24. In Proc. the 9th Int. EMIS Conference, Kiryat Anavim, Israel, May 10-13., 1976
Nucl. Instr. Meth. 139 (1976) 1-364

25. S.W. Yuan, Foundations of Fluid Mechanics; Prentice-Hall, New York, 1967

26. H. Dautet, S. Gujrathi, W.J. Wiesehahn, J.M. D'Auria and B.D. Pate, Nucl. Instr. Meth. 107 (1973) 49

27. S. Dushman, Scientific Foundations of Vacuum Technique, ed. J.M. Lafferty; J. Wiley, New York, 1966

28. N.A. Fuchs, Mechanics of Aerosols; Pergamon Press, New York, London, 1964

29. S. Hillebrand, P. Puumalainen and K. Valli, Nucl. Instr. Meth. 110 (1973) 539

30. K. Hellmuth, S. Hillebrand, P. Suominen, K. Valli and J. Äystö, University of Jyväskylä, Dept. of Physics, Res. Rep. No 4/75 (1975)

31. C.B. Fulmer, Phys. Rev. 139 (1965) B54

32. W. Kauzmann, Kinetic Theory of Gases; W.A. Benjamin Inc., New York, 1966

33. American Institute of Physics Handbook, 2nd ed., ed. E. Gray; McGraw-Hill, New York, 1963

34. K.T. Ewing and K.H. Stern, J. Phys. Chem. 78 (1974) 1998

35. W.-D. Schmidt-Ott, R.L. Mlekodaj and C.A. Bingham, Nucl. Instr. Meth. 108 (1973) 13

36. I. Yaffe and R. Cadle, J. Phys. Chem. 62 (1958) 510

37. K.O. Nielsen, Nucl. Instr. Meth. 1 (1957) 289

38. G. Sidenius, Nucl. Instr. Meth. 38 (1965) 19

39. G. Sidenius, Proc. Int. Conf. on Electromagnetic Isotope Separators and the Techniques of their Applications, Marburg, 1970, p. 423

40. Nuclear Level Schemes A = 45 through A = 257 from Nuclear Data Sheets, Academic Press, 1973

41. Nuclear Data Sheets 13 (1974) No. 2

42. Nuclear Data Sheets 17 (1976) No. 4

43. A. Pakkanen, M. Piiparinen, M. Kortelahti, T. Komppa, R. Komu and J. Äystö, University of Jyväskylä, Dept. of Physics, Res. Rep. No. 2/1977

44. J. Honkanen, M. Kortelahti, J. Äystö, A. Hautojärvi and K. Eskola, Department of Physics, University of Jyväskylä, Annual Report 1976, p. 47